

Lead-Free NaNbO_3 Nanowires for a High Output Piezoelectric Nanogenerator

Jong Hoon Jung,^{†,*,‡} Minbaek Lee,^{†,‡} Jung-Il Hong,[†] Yong Ding,[†] Chih-Yen Chen,^{†,§} Li-Jen Chou,[§] and Zhong Lin Wang^{†,*}

[†]School of Materials Science and Engineering, Georgia Institute of Technology, Atlanta, Georgia 30332, United States, [‡]Department of Physics, Inha University, Incheon 402-751, Republic of Korea, and [§]Department of Materials Science and Engineering, National Tsing-Hua University, Hsinchu 30313, Taiwan. [‡]These authors contributed equally to this work.

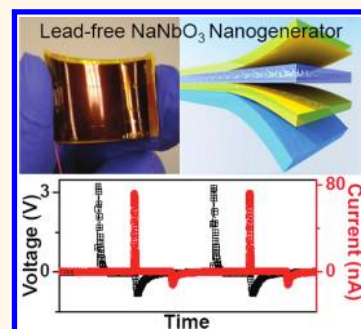
Effective conversion of ubiquitous mechanical energy into electricity is one of the most important issues in the scientific community.^{1,2} In particular, the need for self-powering nanodevices from tiny vibrations such as air pressure and heart beat has inspired the interest for developing high-performance piezoelectric nanomaterials. Until now, piezoelectric ZnO nanowires have been the most outstanding candidate for nanogenerators (NGs).^{3–6} Among piezoelectric materials, displacive ferroelectrics such as lead zirconate titanate exhibit very large piezoelectric coefficients.^{7–9} However, the use of ferroelectric material for harvesting mechanical energy is rare, possibly due to the difficulty in forming one-dimensional nanostructures and the elevated temperature required for the growth.

As for piezoelectric NGs using ferroelectric nanowires, $\text{Pb}(\text{Zr,Ti})\text{O}_3$ and BaTiO_3 have been investigated. Chen *et al.* synthesized $\text{Pb}(\text{Zr,Ti})\text{O}_3$ nanofibers by electrospinning using an output voltage of 1.63 V and an output power of 0.03 μW .¹⁰ Using the aligned $\text{Pb}(\text{Zr,Ti})\text{O}_3$ nanowires grown by a chemical method at relatively low temperature, Xu *et al.* reported an output voltage of 0.7 V and current density of 4 $\mu\text{A}/\text{cm}^2$ and the light up of a commercial LED.¹¹ Park *et al.* synthesized a BaTiO_3 thin film by rf sputtering and fabricated NGs by microfabrication and soft lithographic printing techniques.¹² By bending the flexible substrate, they obtained an output voltage of 1.0 V and a current density of 0.19 $\mu\text{A}/\text{cm}^2$. While the above results are outstanding, we still need a cost-effective device of high output power by using easily accessible and non-toxic ferroelectric nanowires.^{13,14}

In this paper, we report the piezoelectric NGs fabricated using lead-free NaNbO_3

ABSTRACT Perovskite ferroelectric nanowires have rarely been used for the conversion of tiny mechanical vibrations into electricity, in spite of their large piezoelectricity. Here we present a lead-free NaNbO_3 nanowire-based piezoelectric device as a high output and cost-effective flexible nanogenerator. The device consists of a NaNbO_3 nanowire—poly(dimethylsiloxane) (PDMS) polymer composite and Au/Cr-coated polymer films. High-quality NaNbO_3 nanowires can be grown by hydrothermal method at low temperature and can be poled by an electric field at room temperature. The NaNbO_3 nanowire—PDMS polymer composite device shows an output voltage of 3.2 V and output current of 72 nA (current density of 16 nA/cm^2) under a compressive strain of 0.23%. These results imply that NaNbO_3 nanowires should be quite useful for large-scale lead-free piezoelectric nanogenerator applications.

KEYWORDS: lead-free · NaNbO_3 nanowire · high output · piezoelectric nanogenerator



nanowires. A large amount of high-quality NaNbO_3 nanowires can be produced after one reaction at low temperature. By forming a composite of NaNbO_3 nanowires with poly(dimethylsiloxane) (PDMS) polymer, a flexible NG was fabricated easily after applying a direct poling process. Under a compressive strain of 0.23%, we obtained very stable and high output piezoelectric signals, that is, an open circuit voltage of 3.2 V, a closed circuit current of 72 nA, and a power density of 0.6 mW/cm^3 by considering the volume fraction of the NaNbO_3 nanowire inside the PDMS polymer.

RESULTS AND DISCUSSION

There are two different morphologies of NaNbO_3 with nearly the same lattice constant and symmetry (Figure 1). As described

* Address correspondence to zlwang@gatech.edu.

Received for review October 10, 2011 and accepted November 18, 2011.

Published online November 18, 2011
10.1021/nn2039033

© 2011 American Chemical Society

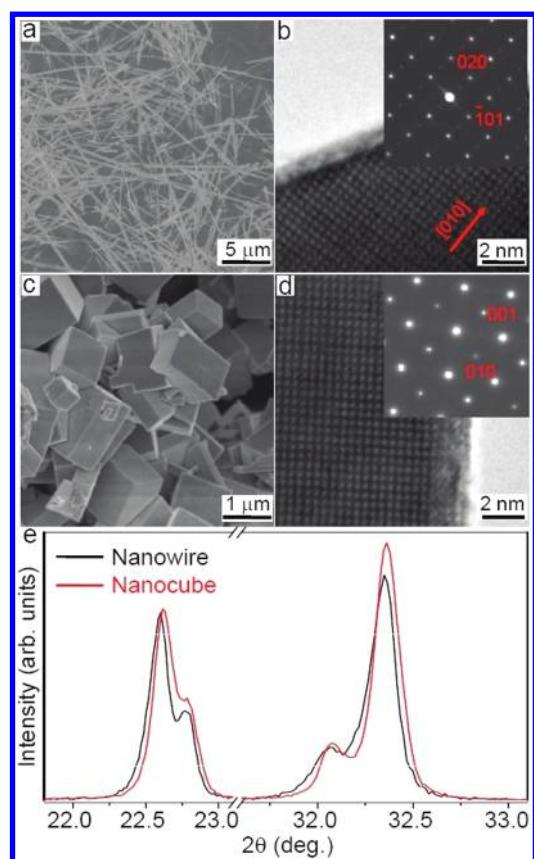


Figure 1. Structural characterization of NaNbO_3 . Scanning electron microscopy (SEM) and transmission electron microscopy (TEM) images of NaNbO_3 nanowire (a,b) and nanocube (c,d). We show the selected area electron diffraction patterns for a nanowire along the [101] zone axis (inset of b) and for a nanocube along the [100] zone axis (inset of d). (e) Comparison of X-ray diffraction patterns for NaNbO_3 nanowire and nanocube.

in the Experimental Methods section, a nanowire is formed at short reaction time and the nanocube is at a long reaction time by a simple hydrothermal method. As-grown $\text{Na}_2\text{Nb}_2\text{O}_6\text{--H}_2\text{O}$ nanowires are successively transformed into NaNbO_3 nanowires with the increase of annealing temperature, as confirmed by *in situ* X-ray diffraction measurement (Supporting Information, Figure S1a).^{15,16} Figure 1a, c shows scanning electron microscopy (SEM) images of nanowires and nanocubes, respectively. The NaNbO_3 nanowires have several tens of micrometers in length and ~ 200 nm diameter. On the other hand, the NaNbO_3 nanocubes have $0.5\text{--}1.0\ \mu\text{m}$ lengths. Figure 1b,d show transmission electron microscopy (TEM) images of a nanowire and a nanocube, respectively. Both nanowires and nanocubes show clear lattice fringes and electron diffraction patterns (insets of Figure 1b,d), suggesting their crystalline quality. Dark-field images show that there are twins along the growth direction for the nanowire and in the facet for the nanocube (Supporting Information, Figure S2). X-ray diffraction and electron diffraction give lattice parameters of $a = 5.567\ \text{\AA}$, $b = 7.764\ \text{\AA}$, $c = 5.515\ \text{\AA}$, and symmetry

of $P2_1ma$ for both annealed nanowires and as-grown nanocubes (Figure 1e).

Having a $P2_1ma$ ferroelectric symmetry rather than $Pbcm$ antiferroelectric symmetry in NaNbO_3 nanostructures is crucial for NG application because the former exhibits large piezoelectricity while the latter does not. Bulk crystalline NaNbO_3 has long been indexed as $Pbcm$ symmetry with $a = 5.506\ \text{\AA}$, $b = 5.566\ \text{\AA}$, and $c = 15.520\ \text{\AA}$ lattice constants.¹⁷ The antiferroelectric $Pbcm$ symmetry is also known to be changed into ferroelectric $P2_1ma$ symmetry by applying an electric field.¹⁸ However, the exceptionally long c -axis has been questioned by several sophisticated experiments.^{19–21} Especially, Shiratori *et al.* reported that the antiferroelectric $Pbcm$ symmetry in bulk changes into the ferroelectric $P2_1ma$ symmetry in submicrometer-sized NaNbO_3 .²² By accepting the interesting size effect in NaNbO_3 nanowires and nanocubes, we further performed the Rietveld analysis for a high-resolution X-ray diffraction pattern (Supporting Information, Figure S1b). The obtained X-ray diffraction results can be better fitted by $P2_1ma$ than $Pbcm$ symmetry, as evidenced by the smaller fitting error.

Having the ferroelectricity (and inherited piezoelectricity) of NaNbO_3 nanowires, we use them for fabricating a NG. Lead-free NaNbO_3 nanowires can be obtained at a relatively large quantity. As shown, the photograph of the obtained nanowires (Figure 2a), one time reaction in a 25 mL sized vessel can produce more than 1.2 g of NaNbO_3 nanowires without any different morphologies and impurities.

Due to the merit of ferroelectricity (piezoelectricity) and the demerit of random alignment, we formed a composite of the NaNbO_3 nanowire and PDMS polymer in a volume ratio of 1:100 to imbue our NGs with flexibility. The piezoelectric device mainly consists of four layers, as schematically shown in Figure 2b. The Au/Cr-coated Kapton films act as top and bottom electrodes, the NaNbO_3 nanowire mixed with the PDMS composite serves as a source of piezoelectric potential, and the thick polyester (PS) film works as a main driving source of strain. Due to the use of all polymer layers in our NG, the device could be bent and released for the generation of electricity (inset of Figure 2b). Top view of NaNbO_3 nanowire–PDMS polymer composite shows that the nanowires were randomly oriented and well-dispersed without aggregations (left panel of Figure 2c). For a $100 \times 100\ \mu\text{m}^2$ area, we observed 150–200 numbers of nanowires. Cross-section view of the device shows a $\sim 100\ \mu\text{m}$ thick NaNbO_3 –PDMS composite (right panel of Figure 2c) in which the upper and lower layers are Au/Cr-coated Kapton films.

Now let us briefly discuss the power generation mechanism. The spontaneous electric dipoles in NaNbO_3 , originated from Nb^{5+} ion movement in NbO_6 octahedra, can have six possible orientations along

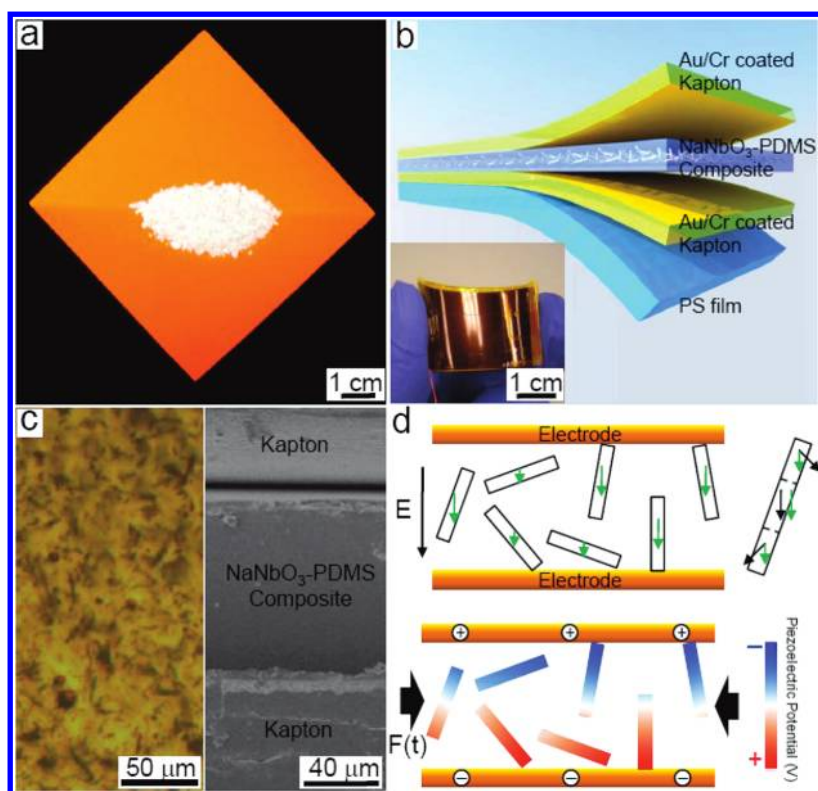


Figure 2. (a) Photograph of obtained NaNbO_3 nanowires after one time reaction. (b) Piezoelectric device scheme. Yellow, blue, and light blue layers correspond to the Au/Cr-coated Kapton film, NaNbO_3 –PDMS composite, and PS film, respectively. We show the photograph of a flexible NG device (inset). (c) Top-view optical microscope (left) and cross-section SEM (right) image of the device. For the top-view image, the upper Kapton film is removed. (d) Schematics of the piezoelectric power generation mechanism. Top: Alignment of dipoles after poling. Individual nanowire has ferroelectric (piezoelectric) domains with different electric dipoles. Each dipole (black arrows) has a component parallel to the electric field (green arrows). For each nanowire, we simply draw the same electric dipole component along the electric field direction. Bottom: Accumulation of free carriers in electrodes after compressive strain (see text for details).

(001) directions. As shown in Figure 1b, the growth direction of the NaNbO_3 nanowire is not parallel to any crystallographic axes. Therefore, the electric dipoles are neither parallel nor perpendicular to the growth direction of the nanowire. Furthermore, the nanowires are randomly oriented inside the PDMS polymer. When the high electric field is applied, the electric dipoles (black arrows) would tend to align along the electric field direction (upper panel of Figure 2d). Some ferroelectric domains (hence piezoelectric domains) will align along the electric field direction, while some domains may tilt from the electric field direction. However, all of the domains have electric dipole components along the electric field direction (green arrows). For each NaNbO_3 nanowire, we simply considered the same electric dipole component along the electric field direction. If we apply a compressive force $F(t)$ parallel to the plane, the NaNbO_3 nanowires are under compressive strain (lower panel of Figure 2d). The strain-induced electric polarization will align to the dipole direction; hence the piezoelectric potential inside the nanowire is higher at the bottom electrode region than at the top electrode region. In order to screen the piezoelectric potential, positive and negative charges will be accumulated at the top and bottom

electrodes, respectively. If the compressive strain is released, the piezoelectric potential should be diminished and the accumulated charges will move back to the opposite direction. Therefore, continuously applying and releasing the compressive strain results in the alternating voltage and current, as similarly discussed in ZnO nanowire-based NGs.^{23,24}

The NaNbO_3 nanowire–PDMS polymer composite is sandwiched by two Kapton films, and a PS supporting film is placed at the bottom. When we bend the piezoelectric device, a strain neutral line is located near the PS film. Therefore, the NaNbO_3 nanowire–PDMS polymer composite is subject to compressive strain. From the given Young's modulus and thickness of each layer, we can calculate the position of the strain neutral line and strain value, as shown in Supporting Information, Figure S3. Since the thickness of the NaNbO_3 nanowire–PDMS polymer composite is not thin enough, there should be a distribution of strain value. To quantitate the value of strain, we determined the strain of the composite as the constant value at the middle of the NaNbO_3 nanowire–PDMS polymer composite layer. Since the Young's modulus of PDMS (360–870 kPa) is smaller than that of NaNbO_3 (80–104 GPa),^{25,26} the actual strain of NaNbO_3 should be quite small

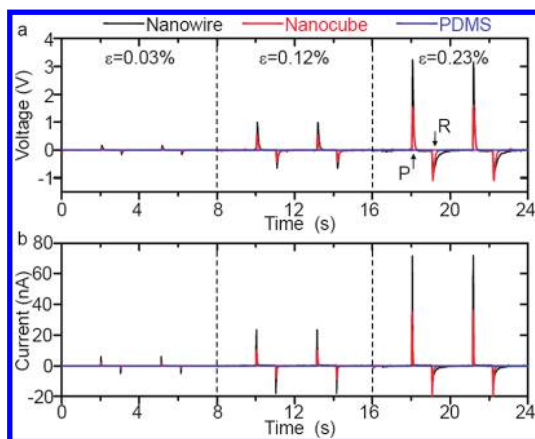


Figure 3. Power generation of NaNbO_3 nanowire-based (black lines) and nanocube-based (red lines) NGs at given compressive strain. (a) Open circuit voltage and (b) closed circuit current. PDMS itself (blue lines) does not show any signals. Here, ϵ , P , and R are for the strain value, press, and release, respectively.

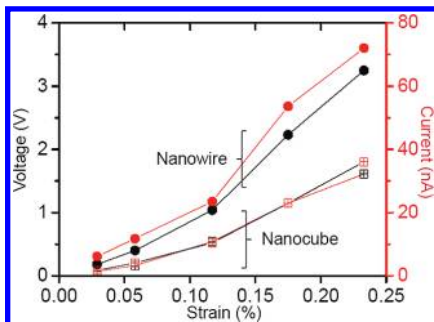


Figure 4. Comparison of generated power for NaNbO_3 nanowire-based (solid circles) and nanocube-based (open cubes) NGs. For all compressive strain values, the output voltage (black symbols) and current (red symbols) of the nanowire-based NG are almost two times larger than those of the nanocube-based NG.

compared with the strain value of the NaNbO_3 –PDMS composite listed in the following.

Figure 3a,b shows the strain dependences of generated open circuit voltage and closed circuit current, respectively. To confirm that the obtained signal comes from the piezoelectricity of NaNbO_3 , we performed the polarity change test (Supporting Information, Figure S4).²⁷ In addition, we observed negligible signals for the device without any electric poling. The generated voltage and current are proportional to the applied strain. The different values of voltage and current between press (P) and release (R) are due to the difference in straining rate when applying and releasing the strain. As clearly seen, for example, the time interval of generated current for press is almost four times shorter than that for release. We confirmed that the area in the current–time curve, which is related to the total transported charges, is nearly the same for pressing and releasing. At the strain value of 0.23% and strain rate of $12.8\% \text{ s}^{-1}$, the output voltage and current (current density) are estimated to

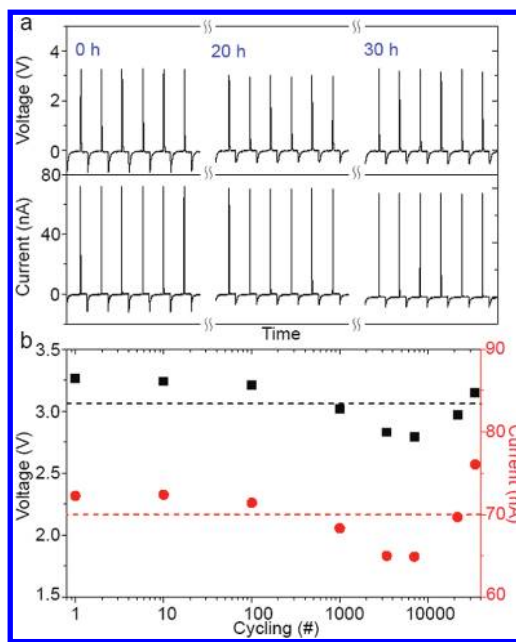


Figure 5. Stability of NaNbO_3 nanowire–PDMS polymer composite piezoelectric NG. Compressive strain ($\epsilon = 0.23\%$) is continuously applied for 30 h with the frequency of 0.33 Hz, *i.e.*, almost 36 000 times. (a) Open circuit voltage and closed circuit current after the given elapsed time. (b) Cycling number dependences of peak values for voltage and current. Dashed lines represent the averaged values.

be $\sim 3.2 \text{ V}$ and $\sim 72 \text{ nA}$ ($\sim 16 \text{ nA/cm}^2$), respectively, which is enough to power a small liquid crystal display (LCD) (Supporting Information, Figure S5). Since the NaNbO_3 nanowire is mixed with PDMS with a volume ratio of 1:100, we can assume that the generated power solely from the NaNbO_3 nanowire is $\sim 0.6 \text{ mW/cm}^3$. These values are higher or comparable to the previous $\text{Pb}(\text{Zr,Ti})\text{O}_3$ - and BaTiO_3 -based piezoelectric device.^{10–12}

To understand the large output power of the NaNbO_3 nanowire-based NGs, we performed two control experiments. First, we tested the power generation only from the PDMS polymer without the NaNbO_3 nanowire. The output voltage and current are negligible under the same experimental conditions (strain, strain rate, and poling voltage). Second, we tested the power generation from a NaNbO_3 nanocube-based NG fabricated using the same procedure. Under the same experimental conditions listed above and the same mixing ratio with PDMS, the output voltage and current from the nanocube-based NG is almost half of that from a nanowire-based NG for all strain values (Figure 4). Since one-dimensional nanowires are superior to zero-dimensional nanocubes in percolation, a nanowire-based NG could effectively deliver generated piezoelectric potentials to the outside electrodes compared to a nanocube-based one.

We tested the stability of the NaNbO_3 nanowire-based piezoelectric NG by continuously applying and releasing the compressive strain. During almost 30 h,

we continuously applied $\sim 36\,000$ cycles of straining. While there is some fluctuations, the output voltage and current are very stable (Figure 5a,b). The mean and standard deviation of output voltage (current) are 3.06 V (70.0 nA) and 0.18 V (3.84 nA), respectively.

There are several merits for the NaNbO₃ nanowire–PDMS composite-based NG. First, a massive production of NaNbO₃ nanowires through wet chemistry and subsequent annealing enables us to fabricate a piezoelectric device at a large scale. Especially, the fact that the NaNbO₃ nanowire does not contain any toxic elements implies further applications like a lead-free nanoactuator. Second, the electric field can effectively pole random piezoelectric domains to one direction due to the ferroelectricity of the NaNbO₃ nanowire. Until now, there have been few reports to align the perovskite ferroelectric nanowire in one direction. Although the NaNbO₃ nanowires are randomly aligned, easy electric poling enables the constructive addition of each piezoelectric signal from an individual nanowire. Large piezoelectric coefficient inherited from the perovskite ferroelectric material is demonstrated to be quite useful for energy harvesting applications. Third, the PDMS polymer may play a role of

preventing the cracking and breaking the NaNbO₃ nanowires upon excessive mechanical straining. It may enable the piezoelectric device to have a very long stability. Fourth, the piezoelectric signal is related to the percolation according to our controlled experiments. Below the breakdown of flexibility, the piezoelectric signal should increase with the volume fraction of the NaNbO₃ nanowire inside the composite polymer.

CONCLUSIONS

In summary, we report the piezoelectric nanogenerator fabricated using a lead-free NaNbO₃ nanowire–PDMS polymer composite. For the 0.23% of compressive strain and the 12.8% s⁻¹ of strain rate, we obtained the 3.2 V of open circuit voltage, the 72 nA of closed circuit current (the 16 nA/cm² of current density), and the 0.6 mW/cm³ of power density by considering the volume fraction of the NaNbO₃ nanowire inside the PDMS polymer. Considering the massive production at relatively low temperature and the easy control of piezoelectric domains by electric field, we conclude that the NaNbO₃ nanowire is a valuable candidate for a nanogenerator.

EXPERIMENTAL METHODS

NaNbO₃ nanowires and nanocubes were synthesized by the hydrothermal method. The 0.24 mol of NaOH (9.6 g, 98%) was dissolved in the 20 mL of distilled water, and then 3.76 mmol of Nb₂O₅ (1 g, 99.99%) was added into the NaOH solution. After stirring for 30 min, the stirred solution was transferred into a 25 mL Teflon-lined stainless steel autoclave to undergo hydrothermal reaction at 150 °C. To obtain nanowires and nanocubes, the reaction was performed for 4 and 10 h, respectively. Obtained white powders were filtered, washed with distilled water, and dried at 80 °C for 12 h. As-grown nanowires were further annealed at 600 °C for 12 h. Annealed NaNbO₃ nanowires were thoroughly mixed with poly(dimethylsiloxane) (PDMS) with the volume ratio of 1:100. (For controlled experiment, we also mixed as-grown NaNbO₃ nanocubes with PDMS at the same volume ratio.) The small amount of mixtures was spin-coated on a Au/Cr-coated Kapton polyimide film at 1000 rpm for 15 s. The 25 nm thick Au and 10 nm thick Cr were deposited on Kapton film by thermal evaporation. Another Au/Cr-coated Kapton film was attached to the surface of the spin-coated NaNbO₃–PDMS composite. The Kapton film sandwiched NaNbO₃–PDMS composite was finally attached to polyester (PS) film. The thicknesses of Kapton and PS films were 125 and 500 μm, respectively. We applied ~ 80 kV/cm of electric field for electric poling at room temperature. Note that electric polarization of the epitaxial NaNbO₃ film is almost saturated above 60 kV/cm.²⁸ A linear motor was used to periodically apply and release the compressive force. We used 0.33 Hz of frequency and changed the bending amplitude. The output signal of the piezoelectric device was recorded by a low-noise voltage and current preamplifiers.

Acknowledgment. We thank the support from BES DOE and NSF. J.H.J. was supported by the National Research Foundation of Korea Grant funded by the Korean Government (NRF-2010-013-C00024).

Supporting Information Available: (1) *In situ* X-ray diffraction pattern and Rietveld analysis, (2) dark-field TEM images,

(3) determination of strain value, (4) polarity change test of piezoelectric signal, (5) powering a small liquid crystal display. This material is available free of charge *via* the Internet at <http://pubs.acs.org>.

REFERENCES AND NOTES

- Dresselhaus, M. S.; Thomas, I. L. *Alternative Energy Technologies*. *Nature* **2001**, *414*, 332–337.
- Wang, Z. L. *Self Powered Nanotech*. *Sci. Am.* **2008**, *298*, 82–87.
- Wang, Z. L.; Song, J. H. Piezoelectric Nanogenerators Based on Zinc Oxide Nanowire Arrays. *Science* **2006**, *312*, 242–246.
- Wang, X. D.; Song, J. H.; Wang, Z. L. Direct-Current Nanogenerator Driven by Ultrasonic Waves. *Science* **2007**, *316*, 102–105.
- Qin, Y.; Wang, X. D.; Wang, Z. L. Microfibre–Nanowire Hybrid Structure for Energy Scavenging. *Nature* **2008**, *451*, 809–813.
- Choi, D.; Choi, M.-Y.; Choi, W. M.; Shin, H.-J.; Park, H. K.; Seo, J.-S.; Park, J.; Yoon, S. M.; Chae, S. J.; Lee, Y. H.; *et al.* Fully Rollable Transparent Nanogenerators Based on Graphene Electrodes. *Adv. Mater.* **2010**, *22*, 2187–2192.
- Suyal, G.; Colla, E.; Gysel, R.; Cantoni, M.; Setter, N. Piezoelectric Response and Polarization Switching in Small Anisotropic Perovskite Particles. *Nano Lett.* **2004**, *4*, 1339–1342.
- Yun, W. S.; Urban, J. J.; Gu, Q.; Park, H. Ferroelectric Properties of Individual Barium Titanate Nanowires Investigated by Scanned Probe Microscopy. *Nano Lett.* **2002**, *2*, 447–450.
- Rørvik, P. M.; Grande, T.; Einarsrud, M.-A. One-Dimensional Nanostructures of Ferroelectric Perovskites. *Adv. Mater.* **2011**, *23*, 4007–4034.
- Chen, X.; Xu, S.; Yao, N.; Shi, Y. 1.6 V Nanogenerator for Mechanical Energy Harvesting Using PZT Nanofibers. *Nano Lett.* **2010**, *10*, 2133–2137.
- Xu, S.; Hansen, B. J.; Wang, Z. L. Piezoelectric-Nanowire-Enabled Power Source for Driving Wireless Microelectronics. *Nat. Commun.* **2010**, *1*, 93.

12. Park, K.-I.; Xu, S.; Liu, Y.; Hwang, G. T.; Kang, S. J. L.; Wang, Z. L.; Lee, K. J. Piezoelectric BaTiO₃ Thin Film Nanogenerator on Plastic Substrates. *Nano Lett.* **2010**, *10*, 4939–4943.
13. Cross, L. E. Materials Science: Lead-Free at Last. *Nature* **2004**, *432*, 24–25.
14. Saito, Y.; Takao, H.; Tani, T.; Nonoyama, T.; Takatori, K.; Homma, T.; Nagaya, T.; Nakamura, M. Lead-Free Piezoceramics. *Nature* **2004**, *432*, 84–87.
15. Zhu, H. Y.; Zheng, Z. F.; Gao, X. P.; Huang, Y. N.; Yan, Z. M.; Zou, J.; Yin, H. M.; Zou, Q. D.; Kable, S. H.; Zhao, J. C.; *et al.* Structural Evolution in a Hydrothermal Reaction between Nb₂O₅ and NaOH Solution: From Nb₂O₅ Grains to Micro-porous Na₂Nb₂O₆·2/3H₂O Fibers and NaNbO₃ Cubes. *J. Am. Chem. Soc.* **2006**, *128*, 2373–2384.
16. Liu, L.; Li, B.; Yu, D.; Cui, Y.; Zhou, X.; Ding, W. Temperature-Induced Solid-Phase Oriented Rearrangement Route to the Fabrication of NaNbO₃ Nanowires. *Chem. Commun.* **2010**, *46*, 427–429.
17. Sakowski-Cowley, A. C.; Lukaszewicz, K.; Megaw, H. D. The Structure of Sodium Niobate at Room Temperature, and the Problem of Reliability in Pseudosymmetric Structures. *Acta Crystallogr.* **1969**, *B25*, 851–865.
18. Ulinzheev, A. V.; Leiderman, A. V.; Smotrakov, V. G.; Topolov, V. Yu.; Fesenko, O. E. Phase Transitions Induced in NaNbO₃ Crystals by Varying the Direction of an External Electric Field. *Phys. Solid State* **1997**, *39*, 972–974.
19. Johnston, K. E.; Tang, C. C.; Parker, J. E.; Knight, K. S.; Lightfoot, P.; Ashbrook, S. E. The Polar Phase of NaNbO₃: A Combined Study by Powder Diffraction, Solid-State NMR, and First-Principles Calculations. *J. Am. Chem. Soc.* **2010**, *132*, 8732–8746.
20. Yan, C.; Nikolova, L.; Dadvand, A.; Harnagea, C.; Sarkissian, A.; Perepichka, D. F.; Xue, D.; Rosei, F. Multiple NaNbO₃/Nb₂O₅ Heterostructure Nanotubes: A New Class of Ferroelectric/Semiconductor Nanomaterials. *Adv. Mater.* **2010**, *22*, 1741–1745.
21. Yuzyuk, Yu. I.; Shakhovoy, R. A.; Raevskaya, S. I.; Raevski, I. P.; Marssi, M. E.; Karkut, M. G.; Simon, P. Ferroelectric Q-Phase in a NaNbO₃ Epitaxial Thin Film. *Appl. Phys. Lett.* **2010**, *96*, 222904.
22. Shiratori, Y.; Magrez, A.; Dornseiffer, J.; Haegel, F.-H.; Pithan, C.; Waser, R. Polymorphism in Micro-, Submicro-, and Nanocrystalline NaNbO₃. *J. Phys. Chem. B* **2005**, *109*, 20122–20130.
23. Zhang, Y.; Liu, Y.; Wang, Z. L. Fundamental Theory of Piezotronics. *Adv. Mater.* **2011**, *23*, 3004–3013.
24. Hu, Y. F.; Zhang, Y.; Xu, C.; Zhu, G.; Wang, Z. L. High-Output Nanogenerator by Rational Unipolar Assembly of Conical Nanowires and Its Application for Driving a Small Liquid Crystal Display. *Nano Lett.* **2010**, *10*, 5025–5031.
25. Egerton, L.; Dillon, D. M. Piezoelectric and Dielectric Properties of Ceramics in the System Potassium–Sodium Niobate. *J. Am. Ceram. Soc.* **1959**, *42*, 438–442.
26. Palatnikov, M. N.; Shcherbina, O. B.; Efremov, V. V.; Sidorov, N. V.; Salak, A. N. Microstructure and Elastic Modulus of Ceramic Li_xNa_{1-x}NbO₃ Perovskite Solid Solutions Prepared at 6 GPa. *Inorg. Mater.* **2010**, *46*, 1348–1352.
27. Yang, R.; Qin, Y.; Dai, L.; Wang, Z. L. Power Generation with Laterally-Packaged Piezoelectric Fine Wires. *Nat. Nanotechnol.* **2009**, *4*, 34–39.
28. Mino, T.; Kuwajima, S.; Suzuki, T.; Kanno, I.; Kotera, H.; Wasa, K. Piezoelectric Properties of Epitaxial NaNbO₃ Thin Films Deposited on (001)SrRuO₃/Pt/MgO Substrates. *Jpn. J. Appl. Phys.* **2007**, *46*, 6960–6963.